Proceedings of the 2018 Joint Rail Conference
JRC2018
April 18-20, 2018, Pittsburgh, PA, USA

JRC2018-6214

DEFECT PROGNOSTICS MODELS FOR SPALL GROWTH IN RAILROAD BEARING ROLLING ELEMENTS

Nancy De Los Santos
Mechanical Engineering Department
The University of Texas Rio Grande Valley
Edinburg, TX 78539, USA
nancy.delossantos01@utrgv.edu

Constantine M. Tarawneh, Ph.D.
Mechanical Engineering Department
The University of Texas Rio Grande Valley
Edinburg, TX 78539, USA
constantine.tarawneh@utrgv.edu

Robert E. Jones, Ph.D.
Mechanical Engineering Department
The University of Texas Rio Grande Valley
Edinburg, TX 78539, USA
robert.jones@utrgv.edu

Arturo Fuentes, Ph.D.
Mechanical Engineering Department
The University of Texas Rio Grande Valley
Edinburg, TX 78539, USA
arturo.fuentes@utrgv.edu

ABSTRACT

Prevention of railroad bearing failures, which may lead to catastrophic derailments, is a central safety concern. Early detection of railway component defects, specifically bearing spalls, will improve overall system reliability by allowing proactive maintenance cycles rather than costly reactive replacement of failing components. A bearing health monitoring system will provide timely detection of flaws. However, absent a well verified model for defect propagation, detection can only be used to trigger an immediate component replacement. The development of such a model requires that the spall growth process be mapped out by accumulating associated signals generated by various size spalls. The addition of this information to an integrated health monitoring system will minimize operation disruption and maintain maximum accident prevention standards enabling timely and economical replacements of failing components. An earlier study done by the authors focused on bearing outer ring (cup) raceway defects. The developed model predicts that any cup raceway surface defect (i.e. spall) once reaching a critical size (spall area) will grow according to a linear correlation with mileage. The work presented here investigates spall growth within the inner rings (cones) of railroad bearings as a function of mileage. The data for this study were acquired from defective bearings that were run under various load and speed conditions utilizing specialized railroad bearing dynamic test rigs owned by the University Transportation Center for Railway Safety (UTCRS) at the University of Texas Rio Grande Valley (UTRGV). The experimental process is based on a testing cycle that allows continuous growth of railroad bearing defects until one of two conditions are met; either the defect is allowed to grow to a size that does not jeopardize the safe operation of the test rig, or the change in area of the spall is less than 10% of its previous size prior to the start of testing. The initial spall size is randomly distributed as it depends on the originating defect depth, size, and location on the rolling raceway. Periodic removal and disassembly of the railroad bearings was carried out for inspection and defect size measurement along with detailed documentation. Spalls were measured using optical techniques coupled with digital image analysis, as well as, with a manual coordinate measuring instrument with the resulting field of points manipulated in MatLab™. Castings were made of spalls using low-melting, zero-shrinkage bismuth-based alloys, so that a permanent record of the spall geometry and its growth history can be retained. The main result of this study is a preliminary model for spall growth, which can be coupled with bearing condition monitoring tools that will allow economical and effective scheduling of proactive maintenance cycles that aim to mitigate derailments, and reduce unnecessary train stoppages and associated costly delays on busy railways.

INTRODUCTION AND BACKGROUND

Roller bearings carry the heavy loads that railcars often encounter in consumer goods transport in the rail industry. Tapered-roller bearings contain one outer ring (cup) and two inner rings (cones) with rollers transferring the load between the two as illustrated in Figure 1. As part of the operational setting, bearing cups are supported on one side by the railcar side frame.

The load path travels from the railcar side frame to the bearing cup through the bearing adapter and from the cup to the cones through the rollers. Due to the bearing cups being fixed, the top 'hemisphere' of the cup is under constant load, and this region is referred to as the 'loaded zone', whereas, the bottom 'hemisphere' of the cup is referred to as the "unloaded zone'. Cones rotate in unison with the axle and wheels, thus, undergoing cyclic unloading and loading as they enter and exit the loaded zone [1].

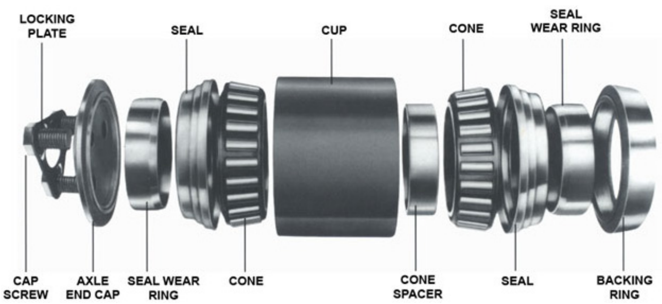

Figure 1. Exploded view of a typical railroad tapered-roller bearing assembly

A common cause of railroad tapered-roller bearing failure is due to rolling contact fatigue (RCF) which can lead to spalling [1]. Based on Hertzian contact mechanics, the highest stresses are located near the surface. As a result of the mechanics of contact loading, the maximum shear stresses occur just below (within 400 micrometers) of the rolling surface [2]. Inclusions located in this region will act as stress risers that maximize the local stress in the steel surrounding the impurity to values well above the endurance limit of the steel. The latter will initiate micro-cracks around the inclusion, which propagate and eventually reach the surface of the component. This damaged region of the surface is known as a 'spall' in a bearing [3]. Spalling will usually occur along the rolling surfaces of the bearing, known as the raceways. When spalls initiate, metallic debris from the failing components is introduced into the bearing's lubricant as well as the dynamic components. The pitting of the rolling surface with the addition of the debris can lead to misalignment of the rollers as they enter the loaded zone. This misalignment increases the friction in the system resulting in higher operating temperatures, which will accelerate the breakdown of the lubricant [4-6]. Additional rolling cycles will cause the bearing to degrade over time. The work presented here investigates the spall size growth in bearing inner rings (cones) that experienced spalling during field and/or laboratory service.

EXPERIMENTAL SETUP AND INSTRUMENTATION

The experiments for this study were conducted utilizing the dynamic bearing testers available at the University of Texas Rio Grande Valley's University Transportation Center for Railway Safety, depicted in Figure 2 through Figure 4.

Figure 2. Older design of the four-bearing tester housed within the environmental chamber showing tester at -40ºC

Figure 3. New design of the four-bearing dynamic tester housed within the environmental chamber

The four-bearing dynamic test rigs (Figure 2 and Figure 3) can accommodate four Class K (6½"×9") or four Class F (6½"×12") tapered-roller bearings mounted onto a test axle. The hydraulic cylinders on these testers are capable of applying various load conditions ranging from 0 to 175% of full load. A fully-loaded railcar or 100% load corresponds to an applied load of 153 kN or 34.4 kips per bearing. An empty railcar corresponds to 17% load which translates to an applied load of 26 kN or 5.85 kips. These four bearing testers feature a 22.3 kW (30 hp) motor that can produce variable bearing rotational speeds that simulate train traveling velocities ranging anywhere from 8 to 137 km/h (5 to 85 mph). To simulate the convection cooling that bearings experience in service which is generated by the air flow passing across the bearing cup, two industrial strength fans were used to produce an airstream traveling across the bearings at an average speed of 18 km/h (11.2 mph). The environmental chamber that houses the four-bearing tester can mimic ambient conditions as low as -40ºC (-40ºF) and as high as 65.6ºC (150ºF).

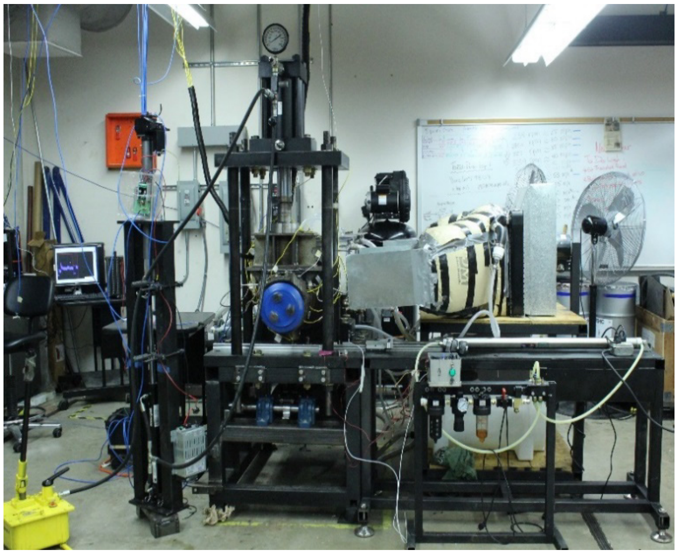

Figure 4. Single Bearing Tester (SBT)

The single bearing tester (SBT) shown in Figure 4 is specially designed to closely replicate the various operating conditions that railroad bearings experience in freight service. This test rig can provide up to 22 kN (5 kips) of lateral load, a variable frequency (0-3 Hz) 70g impact load, in addition to vertical loads of up to 267 kN (60 kips) applied to a single railroad bearing. This tester was used to perform the experiments where the railroad bearings contained large inner ring (cone) spalls and required frequent disassembly and inspection to methodically track the defect (spall) growth.

All the testers are equipped with instrumentation that collects data from the test bearings produced by thermocouples, bayonet thermocouples, 500g high-frequency accelerometers, and the 70g accelerometers devised by the UTCRS research team. Data collected were recorded utilizing a National Instruments (NI) data acquisition system (DAQ) programmed using LabVIEW^{TM}. The NI PXIe-1062Q DAQ is equipped with a NI TB-2627 card to collect temperature data from the thermocouples and an 8-channel NI PXI-4472B card to record the accelerometers were used in this study. The accelerometers were connected to the NI PXI-4472B card via 10-32 coaxial jack and a BNC connection.

METHODOLOGY

The data used for this study were collected from bearings that underwent laboratory service life testing where defect-free cones were run until they developed spalls on the rolling raceways, or from bearings that were removed from field service and found to contain a spall(s) on their inner rings (cones). A total of 11 different cones were run for extended periods of time to generate the data used for this study. Some of the data used in this paper came from a recent publication [3]. The methodology used to collect the data is described in detail in a previous paper by the authors [7].

Figure 5. Casting procedure using Bismuth; (left) spalled surface outlined with tacky tape; (right) Bismuth alloy cast

The data used in this study were acquired from spalls located on the inner rings (cones) of bearings, also referred to as cone spalls. As for the bearing cones that spalled during the laboratory service life testing, once the defect was detected through vibration analysis performed on the acquired accelerometer data, the test was stopped, and the bearing was pressed off, disassembled, cleaned out, and a thorough inspection was carried out. In order to track and maintain accurate records of the spall growth size and to ensure detailed measurements of the spalled area while still allowing testing of the bearing to resume, a casting was made of the spall using low-melting, zero-shrinkage bismuth alloy. Tacky tape is applied around the edges of the defect area to create a mold border for the molten alloy, which melts at 80°C (176°F). The molten bismuth alloy is then poured into the cavity to obtain a casting of the spalled region. This process is pictured in Figure 5.

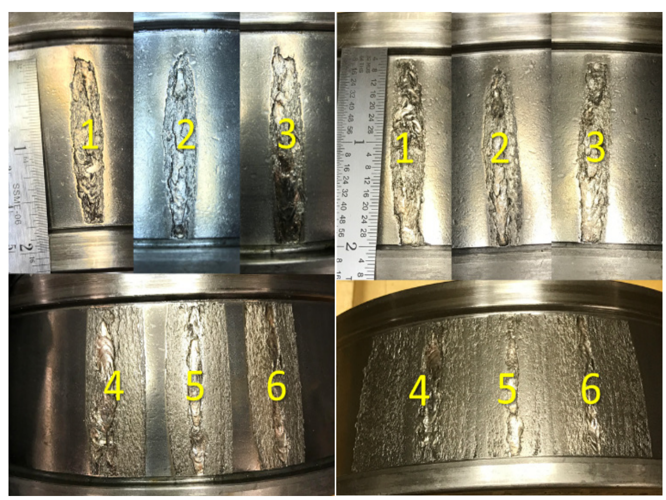

Figure 6. Spall growth in a bearing inner ring (cone) under continued operation (mileage increasing left to right).

Once the casting hardens, it is removed and painted to highlight the borders of the spalled region. The impression is then photographed, and the images are post-processed in MatLab™ to enhance the contrast. The enhanced images are imported to Image Pro-Plus® where measurements of area and other geometric parameters are made. After measurements are taken, the bearings are re-built, re-mounted on the tester, and run under load with periodic removal to carefully track the growth of the initiated spalls. Continuous operation of the defective bearings will result in spall growth, as can be seen in Figure 6. The cone assembly pictured in Figure 6 experienced dramatic growth, as witnessed in the spall size comparisons summarized in Table 1. The listed pre- and post-testing values show growth of more than 12.9 cm^2 (2 in^2) with the merging of spalls 4, 5, and 6 into one larger spalled region.

Note that the experimental results summarized in Figure 8 and Figure 9 reflect total mileage under full-load operation only. However, these bearings also ran for some period of time under loads that simulate an empty railcar as part of other ongoing projects. The empty railcar operation mileage is included in the analysis results presented in Figure 10.

Table 1. Spall size comparison between pre- and post-testing (refer to Figure 6)

Spall No.	Pre-Testing [cm^2] / [in^2]	Post-Testing [cm^2]/[in^2]
1	4.071 / 0.631	4.516 / 0.700
2	3.374 / 0.523	3.935 / 0.610
3	3.555 / 0.551	4.258 / 0.660
4	8.877 / 1.376	40.774 / 6.320
5	9.374 / 1.453	
6	9.252 / 1.434	
Total Spalled Area	38.503 / 5.968	53.483 / 8.290

RESULTS AND DISCUSSION

Tapered-roller bearing spalls will typically grow along the width (laterally) of the rolling raceway until they reach the roller/rib contact area, as can be observed in Figure 6. For the research presented in this paper, the cone spalls have been categorized as: edge (A-B), full-width (C), and centered (D) raceway spalls, as depicted in Figure 7.

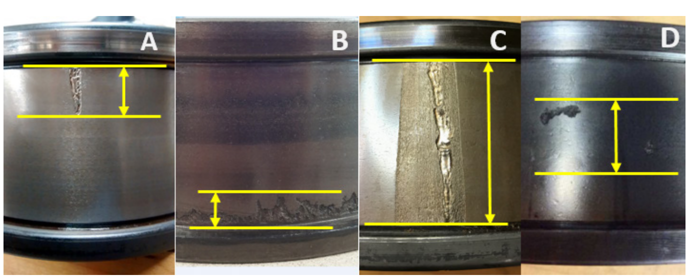

Figure 7. Spall regions for inner rings; (A-B) are classified as edge, (C) full-width, and (D) centered raceway spalls.

In Figure 8, spall area is plotted against the total miles of operation from all previous experiments since the spall was first detected. It is evident that the spall size growth model for spalls located in the middle region of the cone raceway (D) as well as those which span the entire width of the cone raceway (C) will tend to follow one general curve, whereas, spalls located on the edges of the cone raceway (A-B) will follow a much slower growth model. Note that Figure 9 presents the same experimental data used to generate Figure 8 but on a log-log scale. In both figures, the x-value in the provided correlations is in ten-thousands of miles of operation.

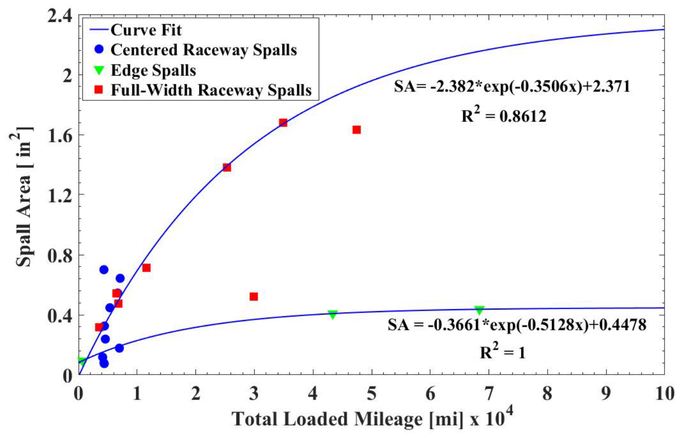

Figure 8. Spall area as a function of the total loaded mileage of operation

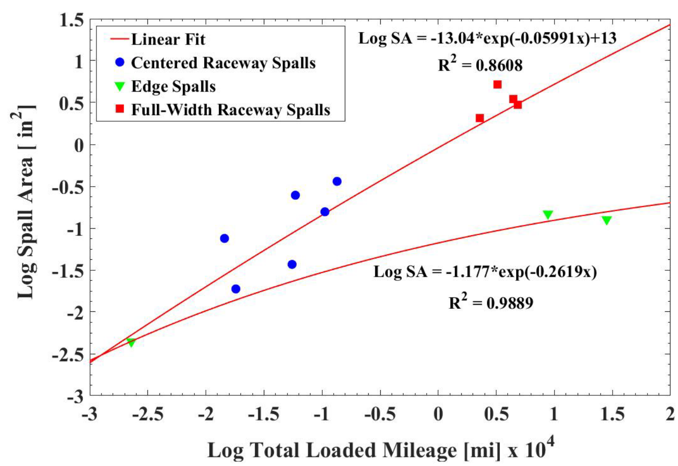

Figure 9. Log spall area as a function of the Log total loaded mileage of operation

For the results shown up to this point, it has been assumed that only operation miles under full-load would produce quantifiable and significant spall growth. Figure 10 presents the spall growth speed as a function of total miles of operation, both loaded (full-load) and unloaded (empty railcar). The figure indicates that there is a poor correlation between spall growth speed and total miles of operation. The spall growth speed correlation provided in Figure 10 represents the best fit curve utilizing all the data points acquired from laboratory testing of bearings with defective (spalled) inner ring (cone) assemblies. Again, the x-value in this correlation is in ten-thousands of miles.

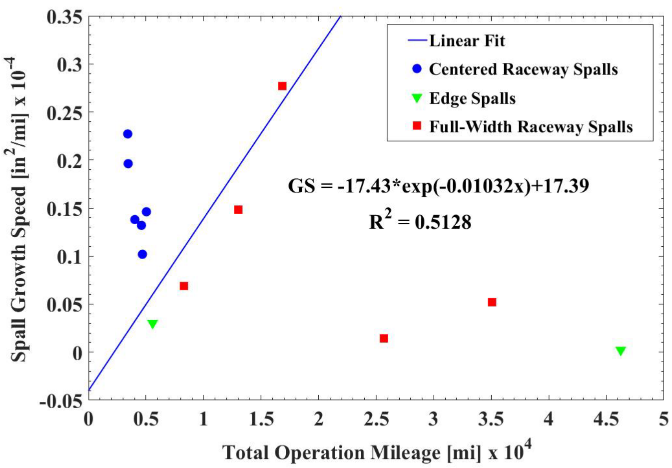

Figure 10. Spall growth rates as a function of the total mileage of operation.

CONCLUSIONS AND FUTURE WORK

The work presented in this paper is a continuation of previous work performed by the authors. In a previous publication [7], the authors presented models that characterize the spall size growth and spall growth speed as a function of miles of operation for railroad bearings containing outer ring (cup) spalls. The work presented here provides spall size growth and spall growth speed models for bearings containing inner ring (cone) spalls.

Several conclusions consistent with that prior work are clear. The first observation is that only mileage under full load is predictive of spall growth. Secondly, this work has shown that there are two growth regimes at play in cone spalls. Spalls forming at the center of the raceway obey a different growth law and grow much more rapidly than spalls which initially form on the cone edges. Thus, the use of a center spall model to predict growth will be conservative for all spall locations. The prior work on cup spalls did not include enough edge spalls to permit a similar insight.

The high fidelity of the fitted models ($R^2 > 0.86$) indicates that this approach has promise for field service application. The very high confidence levels for the edge spall data are not meaningful as there are only three data points, which means fits should be nearly perfect. However, the markedly lower growth rate of edge spalls means that spall location can be safely discounted in using this approach for life prediction and, thus, a higher fidelity edge spall growth model is not essential.

Finally, the results of this study are promising enough that additional data on both cone and cup spalls will be collected to improve confidence in the devised spall growth models. Additionally, all the spall impressions from both cups and cones will be subjected to new analysis using spall volume as a defect measure. Moreover, the area and volume defect measures will be methodically compared to vibration energy signatures of the defective bearings. The ultimate goal of this study is the development of reliable spall growth prognostic models, which can be coupled with bearing condition monitoring systems that will allow economical and effective scheduling of proactive maintenance cycles and mitigate costly catastrophic derailments.

ACKNOWLEDGMENTS

This study was made possible by funding provided by The University Transportation Center for Railway Safety (UTCRS), through a USDOT Grant No. DTRT 13-G-UTC59.

REFERENCES

[1] C. Tarawneh, J. A. Turner, B. M. Wilson, and L. Koester. Service life testing of railroad bearings with known subsurface inclusions detected with advanced ultrasonic technology. *Int. J. of Railway Technology*, Vol. 2, No. 3, pp. 55-78, 2013.

[2] M. A. Mason, C. P. Cartin, P. Shahidi, M. W. Fetty, B. M. Wilson. Hertzian contact stress modeling in railway bearings for assorted load conditions and geometries. *Proceedings of the 2014 ASME Joint Rail Conference*, Colorado Springs, CO, April 2-4, 2014.

[3] C. Tarawneh, L. Koester, A. J. Fuller, B. M. Wilson, and J. A. Turner. Service life testing of components with defects in the rolling contact fatigue zone. *ASTM International*, STP 1548, West Conshohocken, PA, pp. 67-83, 2012.

[4] A. Gonzalez, C. Tarawneh, B. M. Wilson, and J. A. Turner. Tracking of spall deterioration on tapered roller bearing raceways. *Proceedings of the 2015 ASME Joint Rail Conference*, San Jose, CA, March 23- 36, 2015.

[5] B. M. Wilson, A. J. Fuller, C. Tarawneh, and J. A. Turner. Near race inclusions in bearing components and the resultant effect on fatigue initiation and component life. *Proceedings of the 2016 Conference on Railway Excellence (CORE)*, Melbourne, Australia, May 16-18, 2016.

[6] B. M. Wilson, A. J. Fuller, C. Tarawneh, and J. A. Turner. Early bearing fatigue initiation by the identification and selection of bearings with near race defects. *Proceedings of the 2015 International Heavy Haul Association Conference*, Perth, Australia, June 21-24, 2015.

[7] N. De Los Santos, R. Jones, C, Tarawneh, A. Villarreal. Development of prognostic techniques for surface defect growth in railroad bearing rolling elements. *Proceedings of the 2017 ASME Joint Rail Conference*, Philadelphia, PA, April 4-7, 2017.